Photodissociation of Chromium Oxide Cluster Cations

K. S. Molek, Z. D. Reed, A. M. Ricks, and M. A. Duncan*

Department of Chemistry, University of Georgia, Athens, Georgia 30602-2556

Received: May 16, 2007; In Final Form: June 25, 2007

Chromium oxide cluster cations, $Cr_nO_m^+$, are produced by laser vaporization in a pulsed nozzle cluster source and detected with time-of-flight mass spectrometry. The mass spectrum exhibits a limited number of stoichiometries for each value of *n*, where $m > n$. The cluster cations are mass selected and photodissociated using the second (532 nm) or third (355 nm) harmonic output of a Nd:YAG laser. At either wavelength, multiphoton absorption is required to dissociate these clusters, which is consistent with their expected strong bonding. Cluster dissociation occurs via elimination of molecular oxygen, or by fission processes producing stable cation species and/or eliminating stable *neutrals* such as CrO_3, Cr_2O_5, or Cr_4O_{10}. Specific *cation* clusters identified to be stable because they are produced repeatedly in the decomposition of larger clusters include $Cr_2O_4^+$, $Cr_3O_6^+$, $Cr_3O_7^+$, $Cr_4O_9^+$, and $Cr_4O_{10}^+$.

Introduction

Transition metal oxides are used extensively for applications in electronics, catalysis, and magnetic materials.[1−9] The properties of the bulk materials as well as the corresponding nanoparticle and gas-phase cluster oxides have been the subjects of many recent studies. Oxide nanoparticles synthesized by a variety of methods have applications in diverse areas such as solar energy, magnetism, and medicine.[4,10−17] Oxide cluster experiments in the gas phase have contributed fundamental information needed to understand properties such as bonding, reactivity, and structure.[18−39] Theory has been combined with such experiments to probe the structures and stabilities of small clusters.[40−47] Although there are many studies of the mass spectrometry of cluster oxides[18−29] and some investigations of their spectroscopy,[30−39] determining the relative stabilities of these systems remains problematic. In this study of chromium oxide clusters, we address the issue of stability using laser photodissociation of mass-selected cations.

Mass spectrometry has been used extensively to study metal oxide clusters, documenting the stoichiometries formed and relative abundances.[18−29] Unlike the singular "magic numbers" seen for metal carbides,[48−54] metal oxides exhibit several stoichiometries for each metal increment. Extensive studies of the reactivities of transition metal oxides with small hydrocarbons have been reported by Castleman and co-workers.[22] Additional experiments by Bernstein and co-workers have investigated mass distributions using laser photoionization at vacuum ultraviolet wavelengths.[24] In these previous experiments, the patterns of unreactive clusters or those with high abundance were used to infer relative stability. Rare gas matrix isolation[30] and photoelectron spectroscopy of mass selected anions[31−36] have been used to study the spectroscopy of small oxide species. Additional experiments have probed the vibrational spectroscopy of these systems in the far-infrared region using a free electron laser.[37−39] IR-resonance enhanced multiphoton ionization (IR-REMPI) was demonstrated by our group in collaboration with Meijer and co-workers to obtain spectra for several metal carbide[51] and oxide[37] cluster systems. Other work by Fielicke, von Helden, Meijer, and Asmis employed infrared resonance enhanced multiphoton photodissociation (IR-REPD) of mass-selected oxide cation and anion species.[38,39] Theory has also been used to determine structures and spectra of various transition metal oxide clusters.[40−47]

Numerous attempts have been made to experimentally determine the relative stabilities of gas-phase clusters such as metal oxides.[55,56] However, most of these experiments involve some form of mass spectrometry, and problems arise from unknown ionization potentials, fragmentation processes, and size-dependent cross sections. These same issues generally make it difficult to measure the relative concentrations of neutral clusters detected by mass spectrometry, regardless of the ionization method employed. Additional problems arise in cation experiments using energy-variable collision induced dissociation or photodissociation to determine the thresholds for bond breaking. Photoabsorption may not be efficient in the threshold region, and collisional measurements may suffer from significant kinetic shifts, especially for strongly bound clusters. Equilibrium measurements have been performed on the small vanadium oxide clusters,[17] photoionization has been employed on the neutral clusters,[24] collision induced dissociation has investigated various transition metal oxides,[22] and photodissociation has been applied to vanadium, niobium, and tantalum oxides.[21,23] The combined results from these experiments provide evidence for the relative stabilities of some oxide species. Although numerous experiments have studied the vanadium-group oxides, only a few such experiments have considered other transition metal oxide systems.[22]

We have shown previously that mass-selected photofragmentation of metal compound cluster cations is an effective method with which to reveal relative cluster stabilities.[23,49,57] Stable cluster cations are difficult to dissociate and they are produced often as product ions upon the dissociation of larger clusters. Although stable neutral leaving groups are not detected in photodissociation experiments, they can be deduced from the ions that are detected via mass conservation. These methods have been used previously in our lab to study metal carbide clusters[49] and metal−silicon clusters.[57] In a recent study of the

* Corresponding author. E-mail: maduncan@uga.edu. Fax: 706-542-1234.

10.1021/jp073789+ CCC: $37.00
Published on Web 08/01/2007

oxide cluster cations of the vanadium group,[23] we demonstrated that certain cluster stoichiometries are indeed much more stable than others and that other forms of mass spectrometry measurements did not provide a clear picture of these stability patterns. In the present work, we apply this same photodissociation methodology to investigate the chromium oxide cluster system.

Experimental Section

Clusters are produced by laser vaporization in a pulsed nozzle source and mass analyzed in a reflectron time-of-flight spectrometer, as described previously.[23,49,57] The second harmonic (532 nm) of a Nd:YAG laser (Spectra Physics GCR-11) is employed to vaporize material from the surface of a rotating and translating chromium rod. A helium mixture seeded with 1−3% oxygen is pulsed with a General valve (60 psi backing pressure; 1 mm orifice) through the sample rod holder, and oxide cluster cations grow directly from the laser-generated plasma. This molecular beam mixture is expanded in a differentially pumped source chamber and skimmed from there into the detection chamber, where cluster cations are sampled with a reflectron time-of-flight mass spectrometer using pulsed acceleration fields. Pulsed deflection plates in the first flight tube section are used to size-select the clusters of interest before they enter the reflectron. Photoexcitation employs a Nd:YAG laser (DCR-3) at 355 nm, which is timed to intersect the clusters at their turning point in the reflectron field. Subsequently, the parent and fragment ions are mass analyzed in the second drift tube section and detected using an electron multiplier tube and a digital oscilloscope (LeCroy 9310A). Data are transferred from the digital scope to a computer via an IEEE-488 interface. Different studies were performed as a function of laser wavelength and pulse energy for each cluster size. Photodissociation used 20−50 mJ/pulse of unfocused laser beam in a spot size of roughly 1 cm^2.

To investigate the structures and energetics of these metal oxide clusters, geometry optimizations were performed using density functional theory (DFT) computations with the Gaussian 03W program.[58] The Becke-3−Lee−Yang−Parr (B3LYP)[59,60] and Becke-3−Perdew−Wang '91 (B3PW91)[61] functionals were used with the LANL2DZ effective core potential basis set.[62,63] Atomization energies and energies per atom are reported for the minimum energy structures. No symmetry restrictions were placed on the clusters. Minimum energy structures, energies, and vibrations were computed for CrO_3, CrO_3^+, Cr_2O_4, $Cr_2O_4^+$, Cr_2O_5, $Cr_2O_5^+$, Cr_3O_6, $Cr_3O_6^+$, Cr_3O_7, $Cr_3O_7^+$, Cr_4O_{10}, and $Cr_4O_{10}^+$, and these data are reported in the Supporting Information.

Results and Discussion

Mass Spectrometry and Photodissociation. The mass spectrum of $Cr_nO_m^+$ cation clusters produced is shown in Figure 1. Clusters are detected containing up to about 14 metal atoms and varying numbers of oxygen atoms. However, the combining ratios of metal and oxygen are not completely random. Instead, for each metal size, *n*, there are a limited number of stoichiometries seen, where the number of oxygen atoms, *m*, is always greater than *n*. For example, for $n = 4$ the only masses seen are those corresponding to $Cr_4O_9^+$, $Cr_4O_{10}^+$, $Cr_4O_{11}^+$, and $Cr_4O_{12}^+$. A similar trend is seen for all the metal cluster sizes here, giving rise to groups of peaks in the mass spectrum corresponding to the oxides for each metal increment. $Cr_4O_{10}^+$ appears to be anomalous in this spectrum, and indeed this species is found under all conditions to have roughly twice the intensity of any other peak. The cation cluster mass

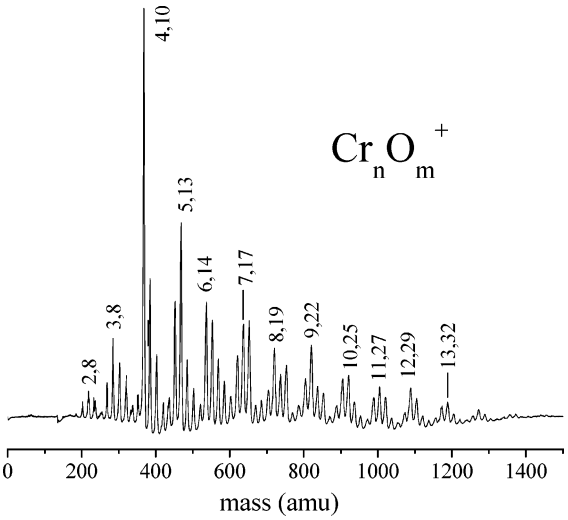

Figure 1. Time-of-flight mass spectrum for $Cr_nO_m^+$ clusters formed in a He expansion.

distribution shown here agrees for the most part with the previous one reported by Castleman and co-workers.[22h] All previous cation mass spectroscopy experiments have noted that the $Cr_4O_{10}^+$ ion was prominent,[22k,28] but it was not found to be quite so pronounced before as we see it here. Mass spectra of partially oxidized $Cr_nO_{1,2}$ clusters were reported by Lievens and co-workers,[26] but these cannot be compared to our data on fully oxidized species. Anion clusters of chromium oxide in this same size range were reported by Castleman and co-workers.[22k]

To investigate the relative stabilities of these various chromium oxide species, we employ mass-selected photodissociation experiments. We select each cluster mass having enough intensity and excite it at 532 and 355 nm to initiate photodecomposition. We find that both wavelengths can induce fragmentation, but that each requires high laser fluences of 20−50 mJ/cm^2 pulse to obtain significant amounts of dissociation. This is consistent with the conditions that we have applied previously to study oxide clusters of the vanadium group,[23] and it indicates that multiphoton excitation is required to break the bonds. The chromium oxide cluster bond energies have been measured via the thresholds for energetic oxidation reactions[29] and they have been calculated with density functional theory.[22k,41,42] These methods suggest that these bond energies are in the range of 3−5 eV, which validates the requirement of multiphoton excitation. Though dissociation is not efficient under any conditions, 355 nm gives the best signals, perhaps because of the greater photon energy or better absorption efficiency at this wavelength. Therefore the data shown throughout this paper are those obtained at 355 nm.

Figures 2−10 show examples of the photofragmentation mass spectra acquired for selected chromium oxide clusters. A complete list of all the cluster ions photodissociated is provided in Table 1 along with the most prominent fragments detected for each of these. The most intense fragments are in bold. The photodissociation mass spectra are collected in a difference mode of operation where the spectrum with the photodissociation laser off (when only the selected parent ion present) is subtracted from that with it on (which contains fragment peaks and undissociated parent ions). This method produces a negative parent ion peak, showing its depletion, and positive fragment ion peaks. Ideally, the integrated intensities of the fragment ion peaks should equal that of the parent ion depletion. However, mass-discrimination effects within our instrument make it impossible to focus on both the parent and fragment ions with

TABLE 1: Stoichiometries of Chromium Oxide Photofragments ($M_nO_m^+ = n, m$) Detected Using 355 nm[a]

parent cation cluster	fragment ions
2,4	2,3; **2,2**; 1,2; **1,1**, Cr^+
2,5	2,4; **2,3**; 1,2; 1,1, Cr^+
2,6	2,5; **2,4**; 2,3; 2,2; 1,2; 1,1, Cr^+
2,7	**2,5**; 2,4; 2,3; 1,2; 1,1, Cr^+
3,5	3,3; 2,6; **2,4**; 2,3; 2,2; 1,2; 1,1; Cr^+
3,6	3,4; 2,4; **2,3**; 2,2; 1,2; **1,1**, Cr^+
3,7	3,5; **2,4**; 2,3; 2,2; 1,2; 1,1, Cr^+
3,8	**3,6**; 2,5; 2,4; **2,3**; 2,2; 1,2; **1,1**, Cr^+
3,9	3,8; 3,7; 3,6; 2,5; **2,4**; 2,3; 2,2; 1,3; 1,2; **1,1**, Cr^+
4,8	2,4; **2,3**; 2,2; 1,2; **1,1**, Cr^+
4,9	3,6; **2,4**; 2,3; 2,2; 1,2; 1,1, Cr^+
4,10	4,8; 3,7; 3,6; 3,5; 2,5; **2,4**; 2,3; 2,2; 1,2; 1,1, Cr^+
4,11	4,10; **4,9**; **3,6**; 2,5; 2,4; 2,3; 1,1
5,12	4,9; 3,7; 3,6; 3,5; **2,4**; 2,3; 2,2; 1,2; 1,1; Cr^+
5,13	4,10; 3,7; 3,6; 3,5; 2,5; **2,4**; 2,3; 2,2; 1,1
6,14	4,9; 4,8; 3,7; 3,6; 3,5; **2,4**; 2,3; 2,2; 1,1
6,15	4,10; 4,9; 3,7; 3,6; 3,5; 2,5; **2,4**; 2,3; 2,2; 1,2; 1,1; Cr^+
6,16	**4,10**; 3,7; 3,6; 3,5; 2,5; **2,4**; 2,3; 1,1; Cr^+
7,16	4,8; **3,6**; 3,5; **2,4**; **2,3**; 2,2; 1,2; 1,1; Cr^+; O^+
7,17	4,10; 4,9; 3,7; 3,6; 3,5; **2,4**; 2,3; 2,2; 1,1; Cr^+
7,18	4,10; 4,9; 3,7; 3,6; 3,5; **2,4**; 2,3; 2,2; 1,1; Cr^+
8,19	**4,9**; 4,8; 3,7; **3,6**; 3,5; **2,4**; 2,3; 2,2; 1,1; Cr^+; O^+
8,20	**4,10**; 4,9; 4,8; 3,7; 3,6; 3,5; 2,4; 2,3; 2,2; 1,1; Cr^+; O^+
8,21	5,12; 4,11; **4,10**; 4,9; 4,8; 3,7; 3,6; 2,4; 2,3
9,21	6,13; **5,11**; 4,9; 4,8; 4,7; **3,6**; 3,5; 2,4; 2,3
9,22	**5,12**; 4,10; 4,9; 4,8; 3,7; **3,6**; 3,5; **2,4**; 2,3; 2,2
9,23	5,12; **4,9**; 4,8; 3,7; 3,6; 3,5; **2,4**; 2,3
9,24	5,13; 5,12; 5,11; **4,10**; 4,9; 4,8; 3,8; 3,7, 3,6; 3,5; 2,5; 2,4; 2,3; 2,2
10,25	6,15; 6,14; 6,13; 5,12; 5,11; **4,10**; 4,9; 4,8; 3,7; **3,6**; 3,5; **2,4**; 2,3
10,26	7,17; 6,15; 6,14; **4,10**; 4,9; 4,8; 3,7; 3,6; 2,4; 2,3
11,27	7,17; 6,14; 6,13; 5,12; 5,11; 4,10; **4,9**; 4,8; 3,7; **3,6**; 3,5; **2,4**; 2,3
12,29	8,18; 7,16; 6,13; 5,12; 5,11; 4,10; **4,9**; 4,8; 3,7; 3,6; 3,5; 2,4; 2,3
13,32	9,22; 7,16; 6,14; 6,13; **5,12**; 5,11; 4,10; **4,9**; 4,8; 3,7; 3,6

[a] The stoichiometries indicated in bold were most prominent.

equal sensitivity.[64] We therefore focus the instrument on the fragment ions and use several different focusing conditions to ensure that no fragments are missed and that no strong bias is present for any mass peaks. For these reasons, we do not report quantitative branching ratios for the various fragment ions observed. Instead, we only distinguish between strong and weak mass peaks. Additionally, in many of our spectra the parent ion peak is presented off-scale. This is so that we can show the more interesting fragment ions in an expanded view.

Figure 2 shows the photodissociation mass spectra for the clusters $Cr_3O_5^+$, $Cr_3O_7^+$, and $Cr_3O_8^+$, hereafter designated as the 3,5; 3,7; and 3,8 species, respectively. As shown, extensive fragmentation is observed, with the formation of product ions containing one, two, or three metal atoms. The 2,4 fragment ion is prominent in all three spectra, as is the lower intensity 1,1 species. The other strong mass peaks (e.g., 2,3 and 3,6 from 3,8) are not repeated in different spectra. It is instructive to first consider those fragments closest in mass to the parent ion because there are fewer possible dissociation channels that might produce these ions. We then find the 3,3 fragment ion from the 3,5 parent, the 3,5 fragment from the 3,7 parent, and the 3,6 fragment from 3,8. In each of these processes, the cluster has eliminated either two oxygen atoms or the diatomic O_2 molecule. The loss of O_2 is the lower energy channel, and because there is little or no signal corresponding to the loss of one oxygen atom, it is perhaps safe to assume that the fragment ions indicated were produced by the elimination of molecular oxygen. This same trend occurs for additional $Cr_3O_m^+$ clusters not shown in this figure. However, in the discussion from this point on, we indicate neutral leaving groups inferred by mass conservation in brackets, e.g., $[O_2]$, to indicate our uncertainty about atomic versus molecular elimination processes.

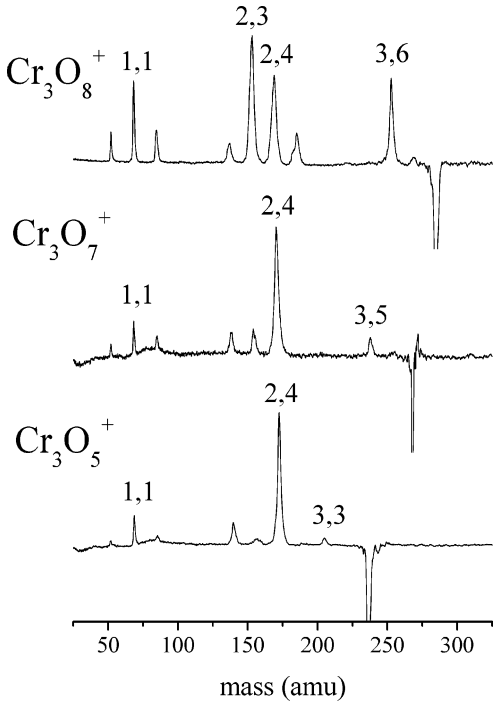

Figure 2. Photodissociation mass spectra of $Cr_3O_m^+$ clusters at 355 nm.

All of the lower mass fragments shown in Figure 2 from all three $Cr_3O_m^+$ clusters could occur through either direct or sequential dissociation processes. In a direct process, the parent ion eliminates the neutral atoms or molecules necessary to conserve mass in one concerted event, whereas in a sequential process the stepwise elimination passes through intermediate fragment ions. For example, the 2,4 fragment from 3,7 could occur directly by the elimination of [1,3] or through the sequence 3,7 → 3,5 → 2,4. On the other hand, the 2,4 ion produced by the fragmentation of 3,5 likely represents a direct process because no intermediate ions are seen that have four oxygens. Sequential processes most likely would go through intermediate ions that also appear in the fragmentation spectrum. However, it is not possible to exclude intermediates that are not detected. These might not appear in the mass spectrum if they have rapid decomposition rates compared to the instrument acceleration time scale (1−2 μs). Laser power or wavelength studies can sometimes reveal the nature of these dissociation mechanisms. However, we find that the dissociation channels seen here are independent of the dissociation laser wavelength (532 vs 355 nm) or laser power (over the range of 1−10 mJ/cm^2 pulse). It therefore remains impossible to distinguish between the possible concerted and sequential processes that might occur here, and this same problem is found throughout this study for all the different cluster sizes. This uncertainty makes it difficult to draw detailed conclusions from the fragmentation spectrum for any one individual cluster. However, as shown in our previous work,[23,49,57] comparing the dissociation spectra for many different cluster sizes makes it possible to detect *patterns* of behavior that do provide new insights. From this point onward, we discuss each cluster size and mention only those dissociation routes that appear to be common to more than one cluster system.

With these considerations in mind, we can identify three patterns in the $Cr_3O_m^+$ data. The ions 1,1 and 2,4 appear in essentially all of these spectra, and are therefore suggested to

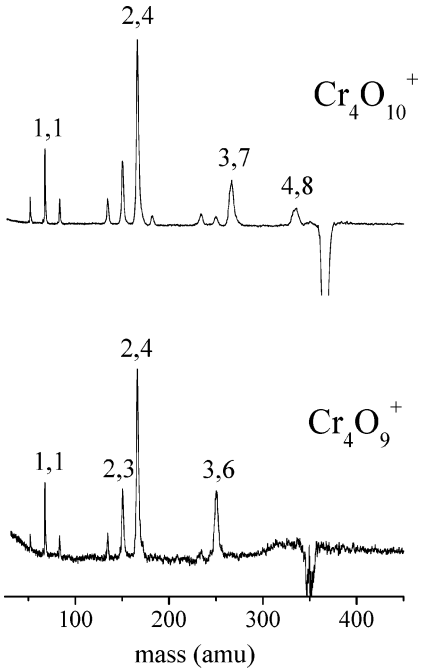

Figure 3. Photodissociation mass spectra of $Cr_4O_m^+$ clusters at 355 nm.

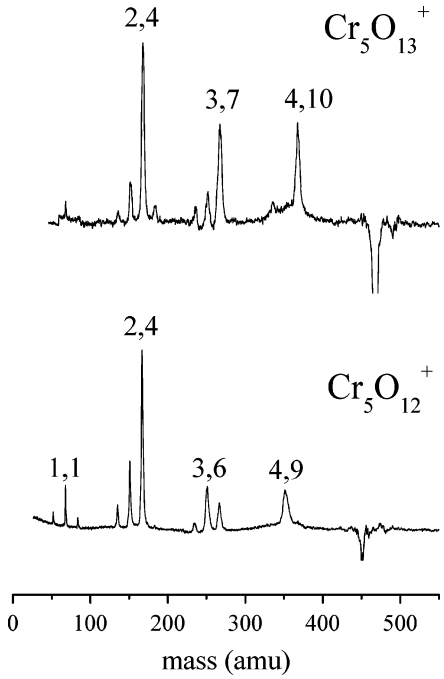

Figure 4. Photodissociation mass spectra of $Cr_5O_m^+$ clusters at 355 nm.

be relatively stable cation clusters. Because of neutral mass differences, we can conclude that $[O_2]$ elimination is common to each of these systems. Finally, the elimination of the neutral [1,3] unit also seems to be important. This is the neutral difference between the strong 2,4 peak and the 3,7 parent. Likewise, if [1,3] is lost from the 3,6 intermediate in the 3,8 spectrum, this would explain the appearance of the 2,3 fragment. The only other time the 2,3 fragment appears in the $Cr_3O_m^+$ data is also by elimination of [1,3] from 3,6 when this species is selected directly as a parent ion (data not shown).

Examples of $Cr_4O_m^+$ fragmentation behavior are presented in Figure 3 and Table 1. The fragmentation of $Cr_4O_{10}^+$ in the figure has a much better signal level than other clusters because the parent ion is so large in the mass spectrum. As shown in the figure, the 2,4 fragment ion is the most intense one in the 4,9 and 4,10 fragmentation spectra, and this also appears prominently in all the 4,*m* spectra, as does the smaller ion 1,1. Neutral $[O_2]$ loss again occurs for some of these clusters. Likewise, the $[CrO_3]$ neutral difference is also common throughout these data. This could explain the sequence of 4,9 → 3,6 → 2,3 and the one of 4,10 → 3,7 → 2,4. It is interesting to note that the $Cr_3O_m^+$ fragments seen are different for the two parent ions shown, and there is a sharp preference for the one that corresponds to [1,3] elimination from the parent. Apparently, the [1,3] loss is more important than the cation stability. However, this argument only applies for $Cr_3O_m^+$ fragments above a certain size. The $Cr_4O_8^+$ parent (data not shown) does not produce a $Cr_3O_m^+$ fragment at all.

The $Cr_5O_m^+$ clusters ($m = 12$, 13), shown in Figure 4, exhibit some of the same patterns seen in the smaller clusters, except that there is no evidence for $[O_2]$ loss. The 2,4 species is again by far the most intense fragment ion observed, and the smaller 1,1 species is also seen. The loss of neutral [1,3] is again apparent throughout the data. As shown in the figure, this could explain the sequence of 5,12 → 4,9 → 3,6 → 2,3 and the additional one of 5,13 → 4,10 → 3,7 → 2,4. The 2,4 ion is seen in situations where it could be formed via a loss of [1,3] units, but it is also seen when this is not possible, indicating its intrinsic stability as a cation. However, the prominent 3,*m* and

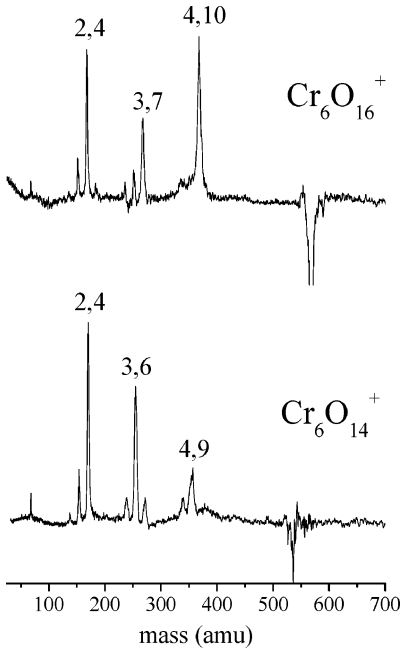

Figure 5. Photodissociation mass spectra of $Cr_6O_m^+$ clusters at 355 nm.

4,*m* fragment ions seen here vary with the parent ion. As shown in the figure, we only see the fragments 3,6 and 4,9 versus 3,7 and 4,10 when they fall in a sequence of [1,3] losses from the parent. The [1,3] leaving group appears to take precedence over the formation of preferred cation fragments in this size range.

The fragmentation of the $Cr_6O_m^+$ clusters ($m = 14$, 16) is shown in Figure 5. As in all the data seen before, the 2,4 fragment ion is among the most prominent. As in the $Cr_5O_m^+$ data, there are 3,7 and 4,10 as well as 3,6 and 4,9 fragments found together from different parents; in both cases the [1,3] difference is apparent. Surprisingly, there are no $Cr_5O_m^+$ fragments detected at all; the fragments closest to the parent ion in mass are the $n = 4$ species. Instead, we find an interval of [2,5] between the $Cr_6O_{14}^+$ parent and the highest mass

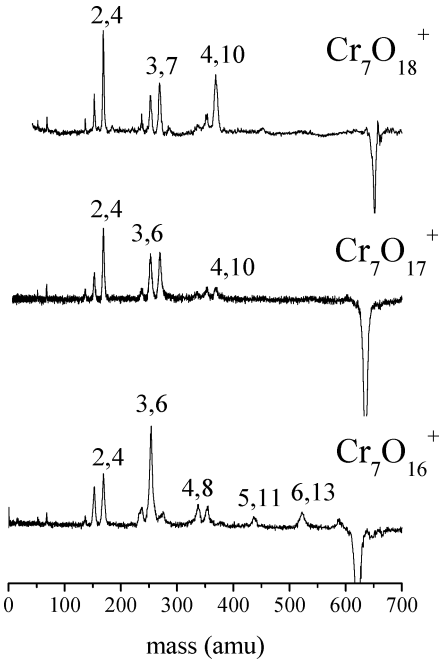

Figure 6. Photodissociation mass spectra of $Cr_7O_m^+$ clusters at 355 nm.

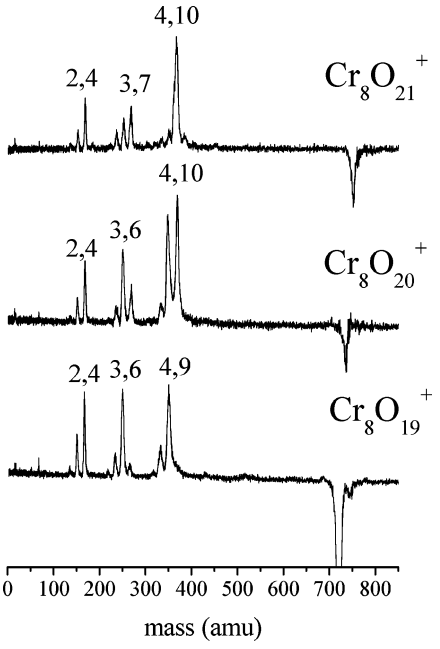

Figure 7. Photodissociation mass spectra of $Cr_8O_m^+$ clusters at 355 nm.

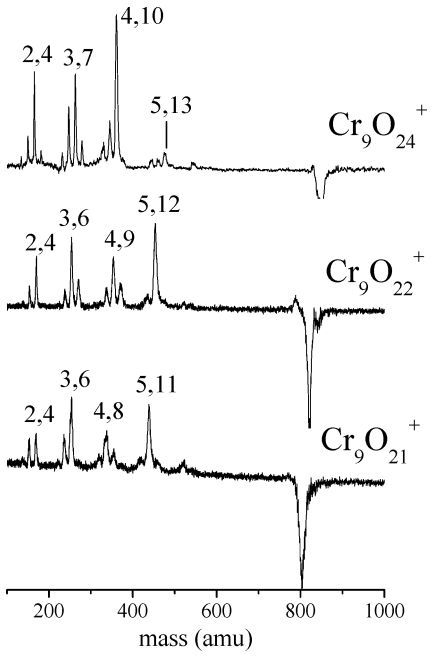

Figure 8. Photodissociation mass spectra of $Cr_9O_m^+$ clusters at 355 nm.

fragment ion, $Cr_4O_9^+$. This is the first evidence for the [2,5] species as a possible leaving group, but as shown later, it also occurs in some of the larger cluster fragmentation channels. The interval between the $Cr_6O_{16}^+$ parent and its highest mass fragment ion, $Cr_4O_{10}^+$ is [2,6], which could of course represent two units of [1,3]. Again, the 4,10 species, which was so prominent in the original cluster distribution grown from the source, is particularly abundant here as a fragment.

Figure 6 shows the fragmentation of the $Cr_7O_{16}^+$, $Cr_7O_{17}^+$, and $Cr_7O_{18}^+$ clusters. As in all the data before, the 2,4 cluster is prominent among the low-mass fragments, as are 3,6 and 3,7. Like the $n = 6$ family of clusters, the 7,17 and 7,18 parents produce no fragments in the $n = 5$ or 6 range, but the 7,16 parent has several here, including 6,13 and 5,11. These fragments can be rationalized because they represent familiar intervals coming from the parent ion ([1,3] and [2,5], respectively). The 4,10 fragment, which has been seen before as a prominent ionized product is only strong here in the decomposition of the 7,18 species. Instead, we find the first evidence for the possible elimination of a 4,10 *neutral* species. The 3,6 fragment seen in the lower trace could come directly from the elimination of [4,10] from the parent 7,16 ion. However, it could also come via the sequence 7,16 → 5,11 → 3,6, which would involve the elimination of two units of [2,5]. In the 7,17 fragmentation, the 3,7 parent could also come from the loss of [4,10]. In the 7,18 fragmentation, the 4,10 cation could come from the elimination of a [3,8] unit, or (perhaps more likely) from the sequential loss of [1,3] and [2,5].

The fragmentation patterns of the $n = 8$ group of clusters (Figure 7) are all quite similar, with no formation of any $n = 5$, 6, or 7 fragment ions. Instead, the highest mass fragments detected are the 4,9 and 4,10 species, which represent about half the mass of each of these parents. It is therefore tempting to imagine a fission process in which these clusters split into two roughly equal pieces. Consistent with this picture, the highest mass fragment from the 8,19 parent is the 4,9 species, which could be formed by the elimination of a single [4,10] or by a sequential elimination of two [2,5] neutrals. However, there is virtually no hint of the possible intermediate fragment masses, and so it seems that direct elimination of neutral [4,10] does perhaps occur. A similar process can explain the formation of the 4,10 fragment ion from the 8,20 parent, but the 4,9 fragment is also seen as a prominent species in this case. In the fragmentation of the 8,21 parent, the most prominent fragment ion seen is the 4,10 species, even though there is no simple loss of neutrals seen before that could go along with this. Therefore, these data, and those present already, indicate that *both* of the 4,9 and 4,10 species are relatively stable as cations. Like the $n = 7$ data, these also suggest that the 4,10 species is a stable neutral leaving group.

Selected examples of data for the $Cr_nO_m^+$ ($n = 9-12$) cluster species are shown in Figures 8−10. These data continue to show many of the same patterns seen already, and can be summarized together. The fragment ions in the small mass range for all of

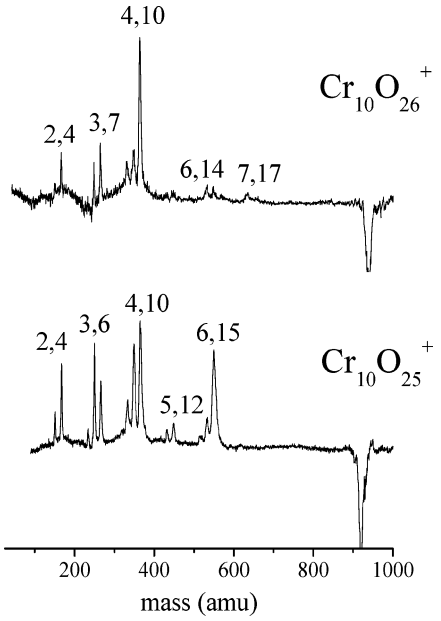

Figure 9. Photodissociation mass spectra of $Cr_{10}O_m^+$ clusters at 355 nm.

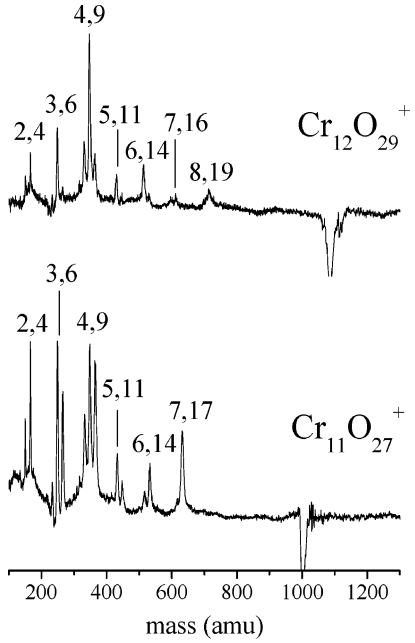

Figure 10. Photodissociation mass spectra of $Cr_{11}O_{27}^+$ and $Cr_{12}O_{29}^+$ clusters at 355 nm.

these continue to be the same species seen already (2,4; 3,6 and 3,7; 4,9 and 4,10). In some cases, such as the fragmentation of the 9,24; 10,26; and 12,29 parents, the 4,9 and 4,10 fragment ions are particularly abundant. However, as the size of the parent ion increases, new cation fragments begin to be observed in the higher mass range. It is understandable that larger pieces would remain when the fragmentation begins at larger clusters, but the specific sizes of these fragments continue to be interesting. In essentially every system, there is a large gap between the parent ion and the nearest high mass fragment ion seen. Moreover, the gap often corresponds to the loss of the [4,10] species. This occurs in the formation of 5,11 from 9,21; 5,12 from 9,22; 6,15 from 10,25; 7,17 from 11,27; and 8,19 from 12,29. In each of these systems, the lower masses that are also seen in these fragmentation patterns more often than not differ from the highest mass fragment by the intervals of [1,3] or [2,5] seen before. In the fragmentation of the 9,21 parent, the highest mass fragment is 5,11, and the next in decreasing mass is 4,8. This 4,8 species is not prominent in other fragmentation patterns, but it differs from 5,11 by the [1,3] interval. Another interesting case is the strong production of 4,9 from the 12,29 parent. This difference corresponds to *two* units of [4,10] neutral loss. It is clear that these common trends of the loss of particular neutral intervals pervade these data. There are no large *cation* species in the size range above $n = 4$ that are produced repeatedly enough to firmly identify them as especially stable.

It is evident from the data presented here that the cation stoichiometries 1,1; 2,4; 3,6; 3,7; 4,9; and 4,10, as well as the neutral stoichiometries 1,3; 2,5; and 4,10 occur repeatedly throughout these fragmentation processes. As in our previous work, we interpret the production of such species from a variety of parent ions and from different dissociation laser conditions (wavelength, power) to indicate the intrinsic relative stability of these clusters. Also consistent with this, some of these same stoichiometries are apparent as abundant species in the distribution of clusters that grew initially from the cluster source (e.g., 4,10). The special cluster neutrals and ions here can be compared to those found earlier for the vanadium group of oxide clusters produced and studied in this same way.[23] For the vanadium, niobium, and tantalum oxides, we found the stable cation stoichiometries to be 1,2; 2,4; 3,7; 4,9; 5,12; 6,14; and 7,17. The neutral species suggested by mass conservation were 1,2 and 2,5. As indicated, many of the stoichiometries seen for the vanadium group of cluster oxides are seen again here. The stable cations and neutrals seen here can be contrasted with our recent results for iron oxide clusters, where 1:1 stoichiometries were seen throughout the data, i.e., species such as 3,3; 4,4; and 5,5.[65] Thus, the oxide clusters of chromium resemble those of the vanadium group more than they do the oxides of iron.

It is informative to consider how the oxide stoichiometries detected here compare to the known bulk-phase oxides of chromium and how the oxidation states implied here compare to those known for chromium in its various compounds. In the case of the vanadium-group oxide clusters, all the prominent stoichiometries could be rationalized in terms of the well-known +4 and +5 oxidation states of those metals. The most common oxidation states of chromium[3] are respectively +3, +6, and +2. Illustrating this, the most common oxide of chromium in the bulk is Cr(III) oxide, Cr_2O_3, which has the corundum structure.[1−3] Cr(IV) oxide (CrO_2) has a rutile structure and is ferromagnetic, whereas Cr(VI) oxide (CrO_3), commonly known as chromic anhydride, is one of the most powerful oxidizers used in organic chemistry.[1−3] The +6 oxidation state for chromium is also found in its well-known chromate (CrO_4^{2-}) and dichromate ($Cr_2O_7^{2-}$) ions.[3] Castleman and co-workers also noted that the +6 oxidation state was favored in the formation of anion clusters, where the stoichiometry pattern Cr_nO_{3n}.[22k] In the clusters seen here, there is strong evidence again for the importance of the +6 oxidation state, as seen in the CrO_3 neutral leaving group eliminated from many of the clusters here. However, there is no obvious tendency for chromium to take on the +3 or +2 oxidation states. We see no evidence for neutral Cr_2O_3 or CrO elimination. The most prominent larger clusters here are those with stoichiometries like $Cr_2O_4^+$, $Cr_3O_7^+$, and $Cr_4O_{10}^{+/0}$. These clusters appear to have an intermediate oxidation state in the +4/+5 range. Oxidation states of +4 or +5 are possible for chromium, but much less common. However, the Cr_4O_{10} species was discussed previously by Castleman and co-workers, and its +5 oxidation state was noted. Another possibility for these

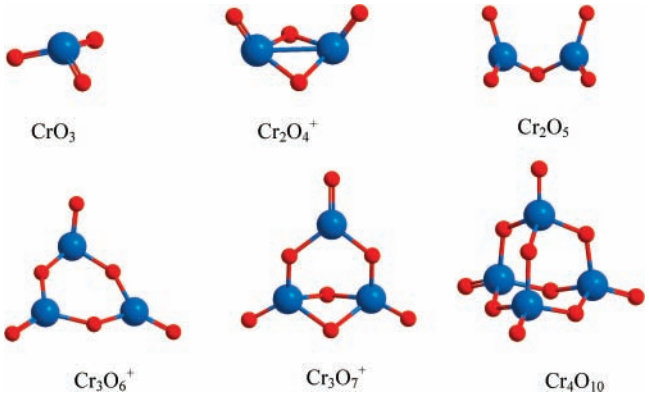

Figure 11. Structures calculated for some of the stable cation and neutral clusters suggested by this work.

systems is that they have mixed valence character. For example, the $Cr_2O_4^+$ ion could be rationalized to have one Cr in the +3 state and the other in the +6 state. Likewise, the $Cr_3O_7^+$ species could conceivably have two +6 metal atoms and one in the +3 state. In pure metal clusters, oxidation states are not usually discussed because charge can be highly delocalized. However, in these metal oxide clusters, localized bonding and charges are possible. We investigate these possible influences on the electronic structure further below. Overall, it is apparent that the most abundant stoichiometries seen here for chromium are more like those of vanadium oxides than they are like those of iron oxides, in direct contradiction to the trends known for oxidation states in the usual compounds of these elements.

Density Functional Theory Calculations. To investigate the reasons for the stability of the specific ions and neutrals identified here, we have performed DFT calculations to explore their structures and binding energies. Previous theoretical work has examined the smaller $Cr_{1,2}O_{1-4}$ species[41] and the stoichiometries found for the anions (including the Cr_4O_{10} neutral),[22k] but there has been no computational study that covers all the neutral and cation species seen here. To consider all of these at the same level of theory, we have re-examined species that were treated previously and extended the theoretical treatment to several new clusters. We have employed the most commonly used B3LYP functional for these calculations but have also explored the B3PW91 functional. A recent study by Dixon and co-workers showed that the former functional has problems for small chromium oxide clusters, whereas the latter provides energetic data judged to be more reliable.[66] We have investigated the stable ions $Cr_2O_4^+$, $Cr_3O_6^+$, $Cr_3O_7^+$, and $Cr_4O_{10}^+$ and the stable neutrals CrO_3, Cr_2O_5, and Cr_4O_{10}. Figure 11 shows the schematic structures determined for these species, and the specific details of these structures are presented in the Supporting Information. For each of these stable ions and neutrals, we have also investigated the corresponding neutrals and ions, respectively, to explore the role of the charge in relative stability. The energetics for these species are summarized in Table 2.

As shown in Figure 11, the structures for all of these oxides involve alternating metal−oxygen−metal networks. This is expected because the structures of the corresponding bulk oxide solids have similar connectivity. Additionally, to balance the greater effective positive charge on the metal, there are so-called terminal oxygen atoms on most of the chromium atoms. Only in the case of the $Cr_2O_4^+$ species is there evidence of metal−metal bonding. As expected, the bond energies for these species are substantial. Table 2 shows that each of these clusters has average per-bond energies in the range 70−90 kcal/mol (3.0−4.0 eV). DFT is perhaps not the best method with which to

TABLE 2: Energetics (kcal/mol) Computed for the Clusters Studied Here

	atomization energy		energy per bond		
	B3LYP	B3PW91	B3LYP	B3PW91	spin multiplicity
CrO_3	455.2	453.1	75.9	75.5	1
CrO_3^+	404.8	314.4	67.5	55.7	2
Cr_2O_4	663.2	652.6	82.9	81.6	1
$Cr_2O_4^+$	613.9	658.9	68.2	73.2	2
Cr_2O_5	813.9	807.6	81.4	80.8	1
$Cr_2O_5^+$	747.2	724.8	74.7	72.5	2
Cr_3O_6	1114.1	1098.8	92.8	91.6	5
$Cr_3O_6^+$	1064.4	1047.9	88.8	87.3	6
Cr_3O_7	1266.0	1255.0	90.4	89.6	5
$Cr_3O_7^+$	1174.1	1163.4	83.9	83.1	6
Cr_4O_{10}	1805.3	1805.3	90.3	90.3	1[a]
$Cr_4O_{10}^+$	1591.1	1738.2	79.6	86.9	4

[a] B3LYP gives a singlet ground state; B3PW91 gives a triplet ground state.

calculate exact bond energies and the numbers obtained for each cluster vary noticeably with the functional employed. Therefore, these bond energetics must be viewed as rough estimates, but it is clear that these systems have strong bonding stability. The relative numbers for these bond energies are also informative when charged versus neutral species are considered. In the case of CrO_3, the neutral, which is seen as a leaving group, does indeed have a greater binding energy than its corresponding ion. The neutral has a closed shell singlet ground state with one of the common bulk stoichiometries and the +6 oxidation state for the metal atom, consistent with previous work.[41] Because it is closed shell, it is not surprising that this neutral is more stable than its corresponding cation. Most of the larger clusters are also somewhat more stable as neutrals than they are as ions. The only possible exception to this is $Cr_2O_4^+$, which has a slightly greater bonding energy as a cation when the B3PW91 functional is employed. As noted above, the 2,4 cation could conceivably take on a mixed-valence structure with the metals in two different oxidation states, having two terminal oxygen atoms connected to one chromium atom, two bridging atoms, and no terminal oxygen on the other chromium atom. However, although we investigated structures such as these, they were not found to be stable minima. Extensive searching and investigation of many other structures led to the species shown here. These are all relatively symmetric structures, in which the metal atoms almost always occupy equivalent sites and thus have the same oxidation states. These effective oxidation states are either +4 or +5 in all the larger clusters. In the case of the 4,10 neutral, which was studied previously with theory, the structure found here is quite close to that reported previously by Castleman, Khanna, and co-workers.[22k] In all of these systems, the neutral and ion with the same stoichiometry have essentially the same structures, differing only because of slight changes in bond distances and angles. This is presumably because these structures already maximize the number of strong metal−oxygen bonds. It should also be noted that many of these neutrals and cations have nonzero spins, as was found previously for the chromium oxide anion clusters.[22k] However, the spin of the ground state is different for several of these clusters with the two different functionals employed, and so a careful examination of this issue is perhaps warranted for future research.

The structures shown here demonstrate that the stable clusters grown for chromium oxides and eliminated by fragmentation represent compact symmetric structures. However, based on our calculated bonding energetics, it is difficult to understand why

the experimental data suggests that these species are more stable than other clusters in the same size range. As noted above, essentially all the neutral species are more stable than their corresponding cations, even though only a few of these neutral are found to be common leaving groups. The 1,3 cluster is understandable, because there is such a large binding preference for this neutral. However, the larger clusters have somewhat similar energetics for ions versus neutrals and for clusters with similar sizes. For example, we can compare the per-bond energy of $Cr_2O_4^+$, which is prominent throughout these systems with the $Cr_2O_5^+$ ion, which is never detected as a major photofragment from any larger clusters. Surprisingly, the 2,5 ion has a greater per-bond binding energy than the 2,4 species (using B3LYP). The 2,4 species has a symmetric compact structure, but the 2,5 cluster, which is more like an open chain, apparently has greater bonding stability. The 3,6 and 3,7 cation species are both found in the experiment, but the calculations indicate that the 3,6 species should be more stable per-bond. Therefore, although the experimental trends for cluster stability are quite clear from our dissociation patterns, the computed energetics for these clusters do not provide much insight to support these trends. This puzzling situation may simply result from the poor energetics provided by DFT treatments. Unfortunately, although higher level treatments could in principle provide better energetics, such computations on the larger clusters here present significant theoretical challenges.

Conclusions

Chromium oxide cluster cations produced by laser vaporization have been investigated with time-of-flight mass spectrometry and mass-selected photodissociation. A limited number of oxide stoichiometries is observed at each cluster size with a specific number of metal atoms. The $Cr_4O_{10}^+$ has an especially large abundance in the cluster distribution produced by the source. Photodissociation of these clusters is only possible via multiphoton excitation, consistent with strong metal oxide bonding. Dissociation produces a number of cation clusters repeatedly from many different parent ions, including CrO^+, $Cr_2O_4^+$, $Cr_3O_6^+$, $Cr_3O_7^+$, and $Cr_4O_{10}^+$, and these clusters are concluded to be significantly more stable than others in the same size region. Likewise, the neutral clusters CrO_3, Cr_2O_5, and Cr_4O_{10} are observed repeatedly as leaving groups from a variety of parent cluster ions, and these are concluded to be stable neutrals. The strong stability of the 4,10 cluster as both a neutral and an ion may be in part attributed to the high symmetry of its structure. The cluster stoichiometries seen here resemble those seen previously for the vanadium-group oxide clusters and are quite different from those seen for iron oxides. The oxidation states implied by these data are most often +4 and +5 for the chromium, which are not common in its solid oxide materials.

Density functional theory computations on these clusters derive structures that are appealing with alternating metal−oxygen−metal networks, which lead to strong bonding stability. However, the detailed comparison of the per-bond energetics for different cluster sizes does not provide as clear and compelling a picture of the most stable clusters as the experiment does. Future theoretical investigations of these systems would be useful. Because of their high intrinsic stability, and potential magnetic properties noted previously,[22k] these systems warrant further investigation for possible isolation as nanocluster materials.

Acknowledgment. We gratefully acknowledge generous support for this work from the Air Force Office of Scientific Research (Grant No. FA9550-06-1-0028).

Supporting Information Available: The Supporting Information for this manuscript includes the full citation for ref 58 as well as the full details for the density functional calculations on the clusters studied here, including optimized geometries, vibrational frequencies, spin multiplicities, and energies. This material is available free of charge via the Internet at http://pubs.acs.org.

References and Notes

(1) Cox, P. A. *Transition Metal Oxides*, Clarendon Press, Oxford, 1992.
(2) Rao, C. N.; Raveau, B. *Transition Metal Oxides*, John Wiley, New York, 1998.
(3) Cotton, F. A.; Wilkinson, G.; Murillo, C. A.; Bochmann, M. *Advanced Inorganic Chemistry*, 6th edition, John Wiley & Sons, New York, 1999.
(4) Hayashi, C.; Uyeda, R.; Tasaki, A., *Ultra-Fine Particles*; Noyes, Westwood, 1997.
(5) Henrich, V. E.; Cox, P. A. *The Surface Science of Metal Oxides*; Cambridge University Press, Cambridge, 1994.
(6) Somorjai, G. A. *Introduction to Surface Chemistry and Catalysis*; Wiley-Interscience, New York, 1994.
(7) Gates, B. C. *Chem. Rev.* **1995**, *95*, 511.
(8) (a) Rainer, D. R.; Goodman, D. W. *J. Mol. Catal. A. Chem.* **1998**, *131*, 259. (b) St. Clair, T. P.; Goodman, D. W. *Top. Catal.* **2000**, *13*, 5. (c) Wallace, W. T.; Min, B. K.; Goodman, D. W. *Top. Catal.* **2005**, *34*, 17. (d) Chen, M. S.; Goodman, D. W. *Acc. Chem. Res.* **2006**, *39*, 739.
(9) (a) Wachs, I. E.; Briand, L. E.; Jehng, J. M.; Burcham, L.; Gao, X. T. *Catal. Today* **2000**, *57*, 323. (b) Chen, Y. S.; Wachs, I. E. *J. Catal.* **2003**, *217*, 468. (c) Wachs, I. E., *Catal. Today* **2005**, *100*, 79. (d) Wachs, I. E.; Jehng, J. M.; Ueda, W. *J. Phys. Chem. B* **2005**, *109*, 2275. (e) Tian, H. J.; Ross, E. I.; Wachs, I. E. *J. Phys. Chem. B* **2006**, *110*, 9593.
(10) Pope, M. T.; Müller, A. *Poloyoxometalate Chemistry From Topology via Self-Assembly to Applications*, Kluwer, Boston, 2001.
(11) Crans, D. C.; Smee, J. J.; Gaidamauskas, E.; Yang, L. Q. *Chem. Rev.* **2004**, *104*, 849.
(12) (a) Rockenberger, J.; Scher, E. C.; Alivisatos, A. P. *J. Am. Chem. Soc.* **1999**, *121*, 11595. (b) Puntes, V. F.; Krishnan, K. M.; Alivisatos, A. P. *Science* **2001**, *291*, 2115. (c) Nolting, F.; Luning, J.; Rockenberger, J.; Hu, J.; Alivisatos, A. P. *Surf. Rev. Lett.* **2002**, *9*, 437. (d) Jun, Y. W.; Casula, M. F.; Sim, J. H.; Kim, S. Y.; Cheon, J.; Alivisatos, A. P. *J. Am. Chem. Soc.* **2003**, *125*, 15981. (e) Casula, M. F.; Jun, Y. W.; Zaziski, D. J.; Chan, E. M.; Corrias, A.; Alivisatos, A. P. *J. Am. Chem. Soc.* **2006**, *128*, 1675.
(13) Ayers, T. M.; Fye, J. L.; Li, Q.; Duncan, M. A. *J. Cluster Sci.* **2003**, *14*, 97.
(14) Roesky, H. W.; Haiduc, I.; Hosmane, N. S. *Chem. Rev.* **2003**, *103*, 2579.
(15) Cushing, B. L.; Kolesnichenko, V. L.; O'Connor, C. J. *Chem. Rev.* **2004**, *104*, 3893.
(16) Kang, E.; Park, J.; Hwang, Y.; Kang, M.; Park, J. G.; Hyeon, T. *J. Phys. Chem. B* **2004**, *108*, 13932.
(17) Fernandez-Garcia, M.; Martinez-Arias, A.; Hanson, J. C.; Rodriguez, J. A. *Chem. Rev.* **2004**, *104*, 4063.
(18) (a) Berkowitz, J.; Chupka, W. A.; Inghram, M. G. *J. Chem. Phys.* **1957**, *27*, 87. (b) Inghram, M. G.; Chupka, W. A.; Berkowitz, J. *J. Chem. Phys.* **1957**, *27*, 569.
(19) Farber, M.; Uy, O. M.; Srivastava, R. D. *J. Chem. Phys.* **1972**, *56*, 512.
(20) Bennett, S. L.; Lin, S. S.; Gilles, P. W. *J. Phys. Chem.* **1974**, *78*, 266.
(21) (a) Kooi, S. E.; Castleman, A. W. *J. Phys. Chem. A* **1999**, *103*, 5671. (b) Bell, R. C.; Zemski, K. A.; Justes, D. R.; Castleman, A. W. *J. Chem. Phys.* **2001**, *114*, 798.
(22) (a) Deng, H. T.; Kerns, K. P.; Castleman, A. W. *J. Phys. Chem.* **1996**, *100*, 13386. (b) Bell, R. C.; Zemski, K. A.; Kerns, K. P.; Deng, H. T.; Castleman, A. W. *J. Phys. Chem. A* **1998**, *102*, 1733. (c) Bell, R. C.; Zemski, K. A.; Castleman, A. W. *J. Cluster Sci.* **1999**, *10*, 509. (d) Zemski, K. A.; Bell, R. C.; Castleman, A. W. *Int. J. Mass. Spectrom.* **1999**, *184*, 119. (e) Zemski, K. A.; Bell, R. C.; Castleman, A. W. *J. Phys. Chem. A* **2000**, *104*, 7408. (f) Zemski, K. A.; Justes, D. R.; Bell, R. C.; Castleman, A. W. *J. Phys. Chem. A* **2001**, *105*, 4410. (g) Zemski, K. A.; Justes, D. R.; Castleman, A. W. *J. Phys. Chem. A* **2001**, *105*, 10237. (h) Zemski, K. A.; Justes, D. R.; Castleman, A. W. *J. Phys. Chem. B* **2002**, *106*, 6136. (i) Justes, D. R.; Mitric, R.; Moore, N. A.; Bonacic-Koutecky, V.; Castleman, A. W. *J. Am. Chem. Soc.* **2003**, *125*, 6289. (j) Justes, D. R.; Moore, N. A.; Castleman, A. W. *J. Phys. Chem. B* **2004**, *108*, 3855. (k) Bergeron, D. E.;

Castleman, A. W.; Jones, N. O.; Khanna, S. N. *Nano. Lett.* **2004**, *4*, 261. (l) Kimble, M. L.; Castleman, A. W. *Int. J. Mass. Spectrom.* **2004**, *233*, 99. (m) Sun, Q.; Rao, B. K.; Jena, P.; Stolcic, D.; Kim, Y. D.; Gantefor, G.; Castleman, A. W. *J. Chem. Phys.* **2004**, *121*, 9417. (n) Kimble, M. L.; Castleman, A. W.; Burgel, C.; Bonacic-Koutecky, V. *Int. J. Mass. Spectrom.* **2006**, *254*, 163. (o) Kimble, M. L.; Moore, N. A.; Johnson, G. E.; Castleman, A. W.; Burgel, C.; Mitric, R.; Bonacic-Koutecky, V. *J. Chem. Phys.* **2006**, *125*. (p) Moore, N. A.; Mitric, R.; Justes, D. R.; Bonacic-Koutecky, V.; Castleman, A. W. *J. Phys. Chem. B* **2006**, *110*, 3015. (q) Reilly, N. M.; Reveles, J. U.; Johnson, G. E.; Khanna, S. N., Castleman, A. W. *Chem. Phys. Lett.* **2007**, *435*, 295.

(23) (a) France, M. R.; Buchanan, J. W.; Robinson, J. C.; Pullins, S. H.; Tucker, J. L.; King, R. B.; Duncan, M. A. *J. Phys. Chem. A* **1997**, *101*, 6214. (b) Molek, K. S.; Jaeger, T. D.; Duncan, M. A., *J. Chem. Phys.* **2005**, *123*.

(24) (a) Foltin, M.; Stueber, G. J.; Bernstein, E. R. *J. Chem. Phys.* **1999**, *111*, 9577. (b) Foltin, M.; Stueber, G. J.; Bernstein, E. R. *J. Chem. Phys.* **2001**, *114*, 8971. (c) Shin, D. N.; Matsuda, Y.; Bernstein, E. R. *J. Chem. Phys.* **2004**, *120*, 4150. (d) Shin, D. N.; Matsuda, Y.; Bernstein, E. R. *J. Chem. Phys.* **2004**, *120*, 4157. (e) Matsuda, Y.; Shin, D. N.; Bernstein, E. R. *J. Chem. Phys.* **2004**, *120*, 4142. (f) Matsuda, Y.; Shin, D. N.; Bernstein, E. R. *J. Chem. Phys.* **2004**, *120*, 4165. (g) Matsuda, Y.; Bernstein, E. R. *J. Phys. Chem. A* **2005**, *109*, 314. (h) Matsuda, Y.; Bernstein, E. R. *J. Phys. Chem. A* **2005**, *109*, 3803. (i) Dong, F.; Heinbuch, S.; He, S. G.; Xie, Y.; Rocca, J. J.; Bernstein, E. R. *J. Chem. Phys.* **2006**, *125*, 164318.

(25) (a) Harvey, J. N.; Diefenbach, M.; Schroder, D.; Schwarz, H. *Int. J. Mass. Spectrom.* **1999**, *183*, 85. (b) Schröder, D.; Schwarz, H.; Shaik, S. *Struct. Bonding* **2000**, *97*, 91. (c) Schröder, D.; Jackson, P.; Schwarz, H. *Eur. J. Inorg. Chem.* **2000**, 1171. (d) Jackson, P.; Fisher, K. J.; Willett, G. D. *Chem. Phys.* **2000**, *262*, 179. (e) Jackson, P.; Harvey, J. N.; Schröder, D.; Schwarz, H. *Int. J. Mass. Spectrom.* **2001**, *204*, 233. (f) Schroder, D.; Engeser, M.; Schwarz, H.; Harvey, J. N. *ChemPhysChem* **2002**, *3*, 584. (g) Engeser, M.; Schlangen, M.; Schroder, D.; Schwarz, H.; Yumura, T.; Yoshizawa, K. *Organometallics* **2003**, *22*, 3933. (h) Engeser, M.; Schroder, D.; Schwarz, H. *Chemistry-a European Journal* **2005**, *11*, 5975. (i) Koszinowski, K.; Schlangen, M.; Schroder, D.; Schwarz, H. *Eur. J. Inorg. Chem.* **2005**, 2464. (j) Feyel, S.; Dobler, J.; Schroder, D.; Sauer, J.; Schwarz, H. *Angew. Chem. Int. Ed. Eng.* **2006**, *45*, 4681. (k) Feyel, S.; Schroder, D.; Rozanska, X.; Sauer, J.; Schwarz, H. *Angew. Chem. Int. Ed. Eng.* **2006**, *45*, 4677. (l) Feyel, S.; Schroder, D.; Schwarz, H. *J. Phys. Chem. A* **2006**, *110*, 2647.

(26) Wang, X.; Neukermans, S.; Vanhoutte, F.; Janssens, E.; Verschoren, G.; Silverans, R. E.; Lievens, P. *Appl. Phys. B. Lasers Opt.* **2001**, *73*, 417.

(27) Fielicke, A.; Rademann, K. *Phys. Chem. Chem. Phys.* **2002**, *4*, 2621.

(28) Aubriet, F.; Muller, J. F. *J. Phys. Chem. A* **2002**, *106*, 6053.

(29) (a) Griffin, J. B.; Armentrout, P. B. *J. Chem. Phys.* **1997**, *106*, 4448. (b) Xu, J.; Rodgers, M. T.; Griffin, J. B.; Armentrout, P. B. *J. Chem. Phys.* **1998**, *108*, 9339. (c) Griffin, J. B.; Armentrout, P. B. *J. Chem. Phys.* **1998**, *108*, 8062. (d) Vardhan, D.; Liyanage, R.; Armentrout, P. B. *J. Chem. Phys.* **2003**, *119*, 4166. (e) Liu, F. Y.; Li, F. X.; Armentrout, P. B. *J. Chem. Phys.* **2005**, *123*.

(30) (a) Chertihin, G. V.; Bare, W. D.; Andrews, L. *J. Chem. Phys.* **1997**, *107*, 2798. (b) Zhou, M. F.; Andrews, L. *J. Chem. Phys.* **1999**, *111*, 4230. (c) Andrews, L.; Rohrbacher, A.; Laperle, C. M.; Continetti, R. E. *J. Phys. Chem. A* **2000**, *104*, 8173.

(31) (a) Fan, J. W.; Wang, L. S. *J. Chem. Phys.* **1995**, *102*, 8714. (b) Wang, L. S.; Wu, H. B.; Desai, S. R. *Phys. Rev. Lett.* **1996**, *76*, 4853. (c) Wu, H. B.; Desai, S. R.; Wang, L. S. *J. Am. Chem. Soc.* **1996**, *118*, 7434. (d) Wang, Q.; Sun, Q.; Sakurai, M.; Yu, J. Z.; Gu, B. L.; Sumiyama, K.; Kawazoe, Y. *Phys. Rev. B* **1999**, *59*, 12672. (e) Gutsev, G. L.; Rao, B. K.; Jena, P.; Li, X.; Wang, L.-S. *J. Chem. Phys.* **2000**, *113*, 1473. (f) Sun, Q.; Sakurai, M.; Wang, Q.; Yu, J. Z.; Wang, G. H.; Sumiyama, K.; Kawazoe, Y. *Phys. Rev. B* **2000**, *62*, 8500. (g) Gutsev, G. L.; Jena, P.; Zhai, H.-J.; Wang, L.-S. *J. Chem. Phys.* **2001**, *115*, 7935. (h) Zhai, H.-J.; Wang, L.-S. *J. Chem. Phys.* **2002**, *117*, 7882. (i) Gutsev, G. L.; Bauschlicher, C. W., Jr.; Zhai, H.-J.; Wang, L.-S. *J. Chem. Phys.* **2003**, *119*, 11135. (j) Zhai, H.-J.; Kiran, B.; Cui, L.-F.; Li, X.; Dixon, D. A.; Wang, L.-S. *J. Am. Chem. Soc.* **2004**, *126*, 16134. (k) Yang, X.; Waters, T.; Wang, X.-B.; O'Hair, R. A. J.; Wedd, A. G.; Li, J.; Dixon, D. A.; Wang, L.-S. *J. Phys. Chem. A* **2004**, *108*, 10089. (l) Zhai, H. J.; Huang, X.; Waters, T.; Wang, X. B.; O'Hair, R. A. J.; Wedd, A. G.; Wang, L. S. *J. Phys. Chem. A* **2005**, *109*, 10512. (m) Zhai, H.-J.; Huang, X.; Cui, L.-F.; Li, X.; Li, J.; Wang, L.-S. *J. Phys. Chem. A* **2005**, *109*, 6019. (n) Huang, X.; Zhai, H. J.; Li, J.; Wang, L. S. *J. Phys. Chem. A* **2006**, *110*, 85. (o) Zhai, H. J.; Wang, L. S. *J. Chem. Phys.* **2006**, *125*, 164315. (p) Zhai, H. J.; Wang, L.-S. *J. Am. Chem. Soc.* **2007**, *129*, 3022.

(32) (a) Wenthold, P. G.; Jonas, K. L.; Lineberger, W. C. *J. Chem. Phys.* **1997**, *106*, 9961. (b) Ramond, T. M.; Davico, G. E.; Hellberg, F.; Svedberg, F.; Salen, P.; Soderqvist, P.; Lineberger, W. C. *J. Mol. Spec.* **2002**, *216*, 1. (c) Ichino, T.; Gianola, A. J.; Andrews, D. H.; Lineberger, W. C. *J. Phys. Chem. A* **2004**, *108*, 11307.

(33) (a) Yang, D. S.; Hackett, P. A. *J. Elec. Spectros. Relat. Phenom.* **2000**, *106*, 153. (b) Yang, D. S. *Coord. Chem. Rev.* **2001**, *214*, 187.

(34) Green, S. M. E.; Alex, S.; Fleischer, N. L.; Millam, E. L.; Marcy, T. P.; Leopold, D. G. *J. Chem. Phys.* **2001**, *114*, 2653.

(35) (a) Pramann, A.; Nakamura, Y.; Nakajima, A.; Kaya, K. *J. Phys. Chem. A* **2001**, *105*, 7534. (b) Pramann, A.; Koyasu, K.; Nakajima, A.; Kaya, K. *J. Phys. Chem. A* **2002**, *106*, 4891. (c) Pramann, A.; Koyasu, K.; Nakajima, A.; Kaya, K. *J. Chem. Phys.* **2002**, *116*, 6521.

(36) Yoder, B. L.; Maze, J. T.; Raghavachari, K.; Jarrold, C. C. *J. Chem. Phys.* **2005**, *122*, 094313.

(37) (a) von Helden, G.; Kirilyuk, A.; van Heijnsbergen, D.; Sartakov, B.; Duncan, M. A.; Meijer, G. *Chem. Phys.* **2000**, *262*, 31. (b) van Heijnsbergen, D.; von Helden, G.; Meijer, G.; Duncan, M. A. *J. Chem. Phys.* **2002**, *116*, 2400. (c) van Heijnsbergen, D.; Demyk, K.; Duncan, M. A.; Meijer, G.; von Helden, G. *Phys. Chem. Chem. Phys.* **2003**, *5*, 2515.

(38) (a) Fielicke, A.; Meijer, G.; von Helden, G. *J. Am. Chem. Soc.* **2003**, *125*, 3659. (b) Fielicke, A.; Meijer, G.; von Helden, G. *Eur. Phys. J. D* **2003**, *24*, 69. (c) Fielicke, A.; Mitric, R.; Meijer, G.; Bonacic-Koutecky, V.; von Helden, G. *J. Am. Chem. Soc.* **2003**, *125*, 15716. (d) Demyk, K.; van Heijnsbergen, D.; von Helden, G.; Meijer, G., *Astron. & Astrophys.* **2004**, *420*, 547.

(39) (a) Asmis, K. R.; Bruemmer, M.; Kaposta, C.; Santambrogio, G.; von Helden, G.; Meijer, G.; Rademann, K.; Woeste, L. *Phys. Chem. Chem. Phys.* **2002**, *4*, 1101. (b) Brummer, M.; Kaposta, C.; Santambrogio, G.; Asmis, K. R. *J. Chem. Phys.* **2003**, *119*, 12700. (c) Asmis, K. R.; Meijer, G.; Bruemmer, M.; Kaposta, C.; Santambrogio, G.; Woeste, L.; Sauer, J., *J. Chem. Phys.* **2004**, *120*, 6461. (d) Asmis, K. R.; Santambrogio, G.; Brummer, M.; Sauer, J. *Angew. Chem. Int. Ed. Eng.* **2005**, *44*, 3122. (e) Janssens, E.; Santambrogio, G.; Brummer, M.; Woeste, L.; Lievens, P.; Sauer, J.; Meijer, G.; Asmis, K. R. *Phys. Rev. Lett.* **2006**, *96*.

(40) (a) Sambrano, J. R.; Andres, J.; Beltran, A.; Sensato, F.; Longo, E. *Chem. Phys. Lett.* **1998**, *287*, 620. (b) Calatayud, M.; Silvi, B.; Andres, J.; Beltran, A. *Chem. Phys. Lett.* **2001**, *333*, 493. (c) Calatayud, M.; Andres, J.; Beltran, A. *J. Phys. Chem. A* **2001**, *105*, 9760. (d) Sambrano, J. R.; Gracia, L.; Andres, J.; Berski, S.; Beltran, A. *J. Phys. Chem. A* **2004**, *108*, 10850. (e) Sambrano, J. R.; Andres, J.; Gracia, L.; Safont, V. S.; Beltran, A. *Chem. Phys. Lett.* **2004**, *384*, 56. (f) Gracia, L.; Andres, J.; Safont, V. S.; Beltran, A. *Organometallics* **2004**, *23*, 730.

(41) (a) Veliah, S.; Xiang, K. H.; Pandey, R.; Recio, J. M.; Newsam, J. M. *J. Phys. Chem. B* **1998**, *102*, 1126. (b) Xiang, K. H.; Pandey, R.; Recio, J. M.; Francisco, E.; Newsam, J. M. *J. Phys. Chem. A* **2000**, *104*, 990.

(42) (a) Reddy, B. V.; Khanna, S. N. *Phys. Rev. Lett.* **1999**, *83*, 3170. (b) Morisato, T.; Jones, N. O.; Khanna, S. N.; Kawazoe, Y. *Comp. Mater. Sci.* **2006**, *35*, 366.

(43) Chakrabarti, A.; Hermann, K.; Druzinic, R.; Witko, M.; Wagner, F.; Petersen, M. *Phys. Rev. B* **1999**, *59*, 10583.

(44) Zimmermann, R.; Steiner, P.; Claessen, R.; Reinert, F.; Hufner, S.; Blaha, P.; Dufek, P. *J. Phys.: Condens. Matter* **1999**, *11*, 1657.

(45) (a) Vyboishchikov, S. F.; Sauer, J. *J. Phys. Chem. A* **2000**, *104*, 10913. (b) Vyboishchikov, S. F.; Sauer, J. *J. Phys. Chem. A* **2001**, *105*, 8588. (c) Vyboishchikov, S. F. *J. Mol. Struc. Theochem.* **2005**, *723*, 53.

(46) Albaret, T.; Finocchi, F.; Noguera, C. *J. Chem. Phys.* **2000**, *113*, 2238.

(47) Gutsev, G. L.; Andrews, L.; Bauschlicher, C. W. *Theo. Chem. Accts.* **2003**, *109*, 298.

(48) (a) Guo, B. C.; Kerns, K. P.; Castleman, A. W. *Science* **1992**, *255*, 1411. (b) Guo, B. C.; Wei, S.; Purnell, J.; Buzza, S.; Castleman, A. W. *Science* **1992**, *256*, 515. (c) Guo, B. C.; Castleman, A. W. *Adv. Met. Semicond. Clusters* **1994**, *2*, 137. (d) Cartier, S. F.; May, B. D.; Castleman, A. W. *J. Phys. Chem.* **1996**, *100*, 8175.

(49) (a) Pilgrim, J. S.; Duncan, M. A. *J. Am. Chem. Soc.* **1993**, *115*, 9724. (b) Pilgrim, J. S.; Duncan, M. A. *J. Am. Chem. Soc.* **1993**, *115*, 6958. (c) Duncan, M. A., *J. Cluster Sci.* **1997**, *8*, 239.

(50) Rohmer, M.-M.; Benard, M.; Poblet, J.-M. *Chem. Rev.* **2000**, *100*, 495.

(51) (a) van Heijnsbergen, D.; von Helden, G.; Duncan, M. A.; van Roij, A. J. A.; Meijer, G. *Phys. Rev. Lett.* **1999**, *83*, 4983. (b) von Helden, G.; van Heijnsbergen, D.; Meijer, G. *J. Phys. Chem. A* **2003**, *107*, 1671.

(52) (a) Gueorguiev, G. K.; Pacheco, J. M. *Phys. Rev. Lett.* **2002**, *88*, 115504. (b) Gueorguiev, G. K.; Pacheco, J. M. *Phys. Rev. B* **2003**, *68*, 241401.

(53) (a) Liu, P.; Rodriguez, J. A.; Hou, H.; Muckerman, J. T. *J. Chem. Phys.* **2003**, *118*, 7737. (b) Liu, P.; Rodriguez, J. A.; Muckerman, J. T. *J. Chem. Phys.* **2004**, *121*, 10321. (c) Liu, P.; Lightstone, J. M.; Patterson, M. J.; Rodriguez, J. A.; Muckerman, J. T.; White, M. G. *J. Phys. Chem. B* **2006**, *110*, 7449.

(54) (a) Varganov, S. A.; Gordon, M. S. *Chem. Phys.* **2006**, *326*, 97. (b) Varganov, S. A.; Dudley, T. J.; Gordon, M. S. *Chem. Phys. Lett.* **2006**, *429*, 49.

(55) *Clusters of Atoms and Molecules, Vol. I*, Haberland, H., Ed., Springer, Berlin, 1995. *Clusters of Atoms and Molecules, Vol. II*, Haberland, H., Ed., Springer, Berlin, 1995.

(56) Johnston, R. L. *Atomic and Molecular Clusters*; Taylor & Francis, London, 2002.

(57) (a) Ticknor, B. W.; Duncan, M. A. *Chem. Phys. Lett.* **2005**, *405*, 214. (b) Jaeger, J. B.; Jaeger, T. D.; Duncan, M. A. *J. Phys. Chem. A* **2006**, *110*, 9310.

(58) Frisch, M. J. et al., *Gaussian 03 (Revision B.02*); Gaussian, Inc.: Pittsburgh, PA, 2003.

(59) Becke, A. D. *J. Chem. Phys.* **1993**, *98*, 5648.

(60) Lee, C.; Yang, W.; Parr, R. G. *Phys. Rev. B* **1988**, *37*, 785.

(61) Perdew, J. R.; Chevary, J. A.; Vosko, S. H.; Jackson, K. A.; Pederson, M. R.; Singh, D. J.; Fiolhais, C. *Phys. Rev. B* **1992**, *46*, 6671.

(62) Dunning, T. H.; Hay, P. J. *Methods of Electronic Structure Theory*, Vol. 2, H. F. Schaefer, ed., Plenum Press, 1977.

(63) (a) Hay, P. J.; Wadt, W. R. *J. Chem. Phys.* **1985**, *82*, 270. (b) Hay, P. J.; Wadt, W. R. *J. Chem. Phys.* **1985**, *82*, 284. (c) Hay, P. J.; Wadt, W. R. *J. Chem. Phys.* **1985**, *82*, 299.

(64) Cornett, D. S.; Peschke, M.; LaiHing, K.; Cheng, P. Y.; Willey, K. F.; Duncan, M. A. *Rev. Sci. Instrum.* **1992**, *63*, 2177.

(65) Molek, K. S.; Anfuso, C.; Duncan, M. A. work in progress.

(66) Dixon, D. A. Private communication.